

Michael R. Bruesewitz, R.T.(R)¹, Cynthia H. McCollough, Ph.D.¹, Natalie N. Braun, B.S.¹, Andrew N. Primak, Ph.D.¹,
Joel G. Fletcher, M.D.¹, Bernhard Schmidt, Ph.D.², Thomas Flohr, Ph.D.²

¹CT Clinical Innovation Center, Department of Radiology, Mayo Clinic, Rochester, MN; ²Siemens Medical Solutions, Forchheim, Germany

What is Dual Energy CT

In CT imaging, materials having different chemical compositions can be represented by the same, or very similar, CT numbers, making the differentiation and classification of different types of tissues extremely challenging. A classical example is the difficulty in differentiating between calcified plaques and iodine-containing blood. Although these materials differ in atomic number considerably, depending on the respective mass density or iodine concentration, the bone and iodinated blood may appear identical. In addition to the difficulty in differentiating and classifying tissue types, the accuracy with which material concentration can be measured is degraded by the presence of multiple tissue types. For example, when measuring the amount of iodine enhancement of a soft tissue lesion, the measured mean CT number over the lesion reflects not only the enhancement due to iodine, but also the CT number of the underlying tissue.

The reason for these difficulties in differentiating and quantifying different tissue types is that the measured CT number of a voxel is related to the linear attenuation coefficient $\mu(E)$, which is not unique for any given material but is a function of the material composition, the photon energies interacting with the material, and the mass density of the material. As can be seen in Figure 1, the same values of linear attenuation coefficient can be obtained for two different materials (e.g., iodine and bone) at a given energy, depending on the mass densities.

In dual energy CT, an additional attenuation measurement is obtained at a second energy, allowing the differentiation of the two materials (Figure 1). Assuming the use of monoenergetic x-rays, at approximately 100 keV, the same linear attenuation coefficients are measured for bone and iodine. Data acquired at approximately 40 keV would allow the differentiation of the two materials, regardless of their respective densities. Although medical x-ray tubes generate a polychromatic spectra, the general principle remains valid. Thus, dual energy CT can be defined as the use of attenuation values acquired with different energy spectra, and the known changes in attenuation between the two spectra, in order to differentiate and classify tissue composition.

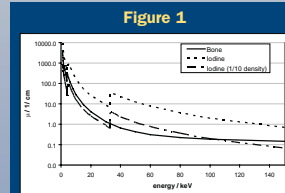


Figure 1
Linear attenuation coefficients for bone (assuming $\rho = 1\text{g/cm}^3$), iodine (assuming $\rho = 0.1\text{g/cm}^3$) and iodine with lower density (assuming $\rho = 0.1\text{g/cm}^3$). Since the linear attenuation coefficient is determined by the mass attenuation coefficient and the density, the same value for $\mu(E)$ can be attained although the materials are different.

New Approaches for Dual Energy CT Using Dual Source CT Systems

Dual source CT is a CT system where two x-ray sources and two data acquisition systems are mounted on the same x-ray gantry, positioned orthogonally to one another on the gantry.¹⁶ A commercial dual source CT system was introduced in 2006 (SOMATOM Definition, Siemens Medical Solutions) and is shown in Figures 2A & B. Each x-ray source is equipped with an independent high-voltage generator, allowing independent control of both the x-ray tube potential and tube current. Although the raw projection data are 90° out of phase, reconstructed images using 360° of projection data are not affected by the phase offset. Thus, simultaneously acquired low- and high-energy images can be reconstructed with comparable image noise levels. Image-based post-processing is then used to extract the dual energy information.

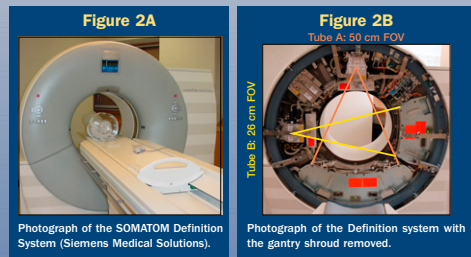


Image-Based Dual Energy CT Techniques

The simplest method for combining the dual energy image data for the purpose of material differentiation is to perform a linearly weighted image subtraction. The low tube potential images (typically 80 kV) are multiplied by a weighting factor and subtracted from the high voltage images (140 kV) to suppress or enhance a specific material.⁷ Alternatively, the CT numbers for low- and high-energy voxels can be combined to produce a dual energy index (u), where:

$$u = \frac{CT_{low} - CT_{high}}{CT_{low} + CT_{high} + 2000 \text{ HU}}$$

This allows the estimation of effective atomic mass numbers, and hence, chemical composition, with water having a value of 0. The dual energy index allows the identification of pure materials up to an atomic number of 55.

Finally, reconstructed images acquired using two different tube potentials can be processed with a three-material decomposition algorithm.⁸ The principle of this technique is illustrated in Figure 3, where the typical CT numbers of three materials of known density are plotted on a graph where the y axis is the CT number at 140 kV and the x axis is the CT number at 80 kV. Ideally, the three materials should be sufficiently different as to create a triangle in this plot. Thereafter, corresponding CT number pairs from the low- and high-energy images are mapped onto the calibration diagram. Depending on their position in the diagram, the material or percent composition of a certain material is determined. The voxels can be color coded according to the percent composition of certain materials or specific materials can be either suppressed or enhanced, depending on the desired clinical application.

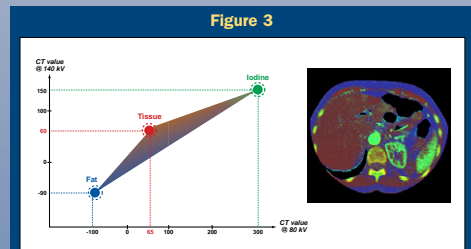


Figure 3
Principle of three material decomposition: for each pixel, the CT numbers for the low- and high-voltage images are mapped into a high- vs. low-voltage CT number diagram. Preadefined values for fat, tissue and iodine mark areas of known material types. The location of a certain pixel-pair in the resulting triangle determines the contribution of a certain material to a respective volume element. The parameters can be altered to differentiate between any three appropriately different materials, for example tissue, fat and calcium or tissue, iodine and xenon.

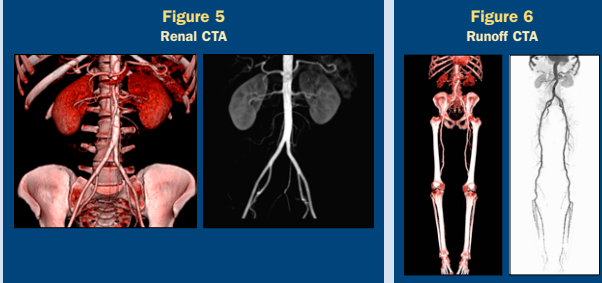
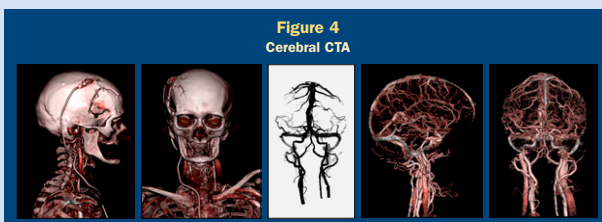
Clinical Applications of Image-Based, Dual-Source, Dual-Energy CT

The dual energy software tools (SyngoDE) for the Siemens Definition became commercially available in March 2007, with an initial focus on the following three clinical tasks: Iodine Imaging, Iodine Removal, and Material Characterization.

Iodine Imaging

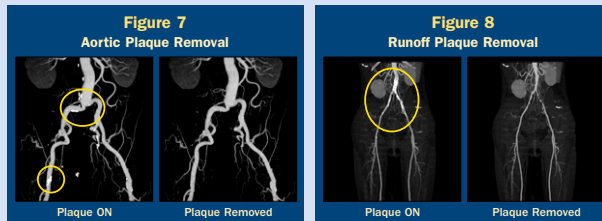
Automated Bone Removal in CT Angiography

One of the most quickly adopted applications of dual energy CT is that of direct CT angiography. In this approach, the dual energy algorithm identifies and removes bone, allowing direct visualization of iodinated vessels. For vessels outside the 26 cm field of view of Tube B, single energy bone removal algorithms are applied to the Tube A data in order to remove large bony anatomy in the periphery of the patient. Examples of this application are shown in Figures 4-6.



Plaque Removal

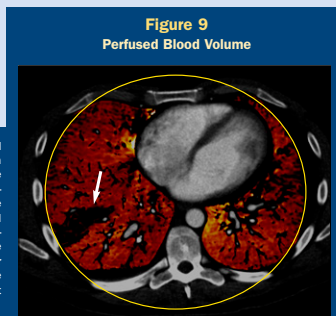
An extension of the bone removal algorithm is a tool to remove not just large bony anatomy, but also discrete hard plaques, potentially allowing clearer visualization of patent lumens in maximum intensity projections. Examples of this application are shown in Figures 7-8.



Perfused Blood Volume (Blood Pool Imaging)

In addition to removing bone to see iodine, the identification of iodine voxels allows for color enhancement of iodinated areas. One potential clinical use is visualization of the perfused blood volume, also referred to as blood pool imaging. An example of this application is shown in Figure 9.

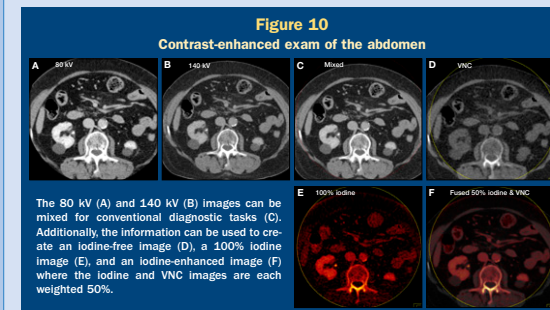
The pulmonary emboli in this patient results in focal perfusion deficit (arrow), which shows up as black in the dual energy image. This tool color codes only the lung tissue, allowing a mixed display where the morphological data of the vasculature is preserved. Tissue outside of the 26 cm FOV of tube B, which is identified by the yellow circle, can not be assessed with the perfused blood volume algorithm. This is not a time resolved perfusion image, requiring multiple scans over time, but rather a display of the iodine content of the lung at the time of the scan, which reflects the amount of blood being supplied to the tissue.



Iodine Removal

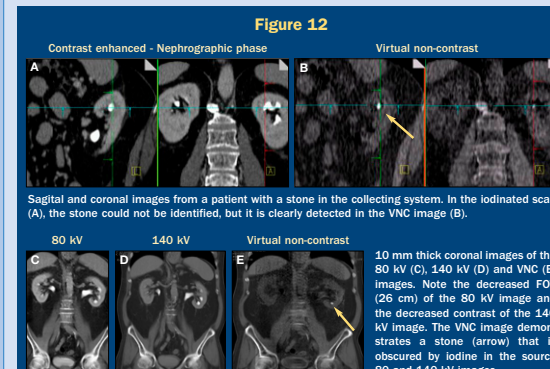
Virtual Non-Contrast (VNC) Images

Another potential application for dual energy CT is, after identifying iodine voxels, to remove the iodine component of the CT number in order to create a "virtual non-contrast image." For applications where the virtual non-contrast image is of sufficient quality to replace the pre-contrast scan, this application can substantially reduce patient dose. Examples of VNC images are shown in Figures 10 - 11.



Dose Reduction

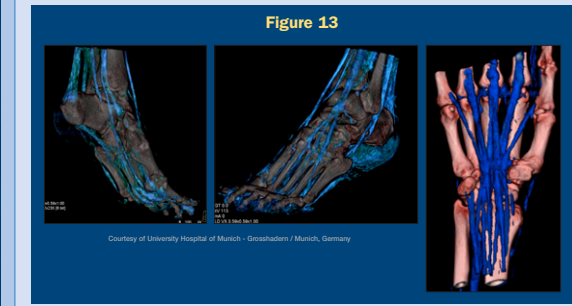
Our present CT urography examination is comprised of only two scans: a pre-contrast scan and combined nephrographic/excretory phase (implemented using a split-bolus). Results to date indicate that the use of a dual energy virtual non-contrast image for the purpose of stone detection may be sufficiently accurate to allow the omission of the pre-contrast scan. This would reduce the patient dose of our current protocol by 50%. The example shown in Figure 12 demonstrates the use of the dual energy virtual non-contrast image for the purpose of stone detection using a contrast-enhanced dual energy dataset.



Material Characterization

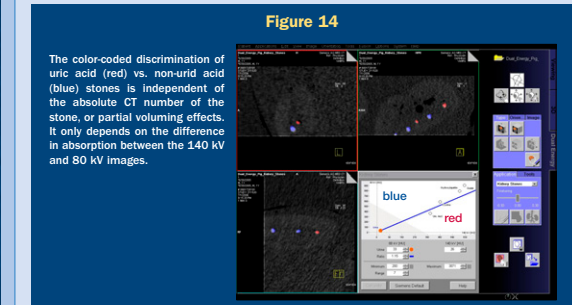
Ligaments and Tendons

Several clinical applications exist where neither bone nor iodine are of interest. Dual energy CT may be useful in identifying different tissue types. One potential application is the visualization of tendons and ligaments, as shown in Figure 13.



Stone Characterization

Experiments performed in vitro using human kidney stones have demonstrated the ability of dual energy material decomposition to discriminate between uric acid and non-uric acid stones.⁹ Clinically, this is an important application, since in vitro determination that a stone is made of uric acid would allow immediate initiation of urinary alkalinization, thereby avoiding the need for further medical testing, or surgical or shockwave interventions. We have validated the accuracy of this approach in phantom models, demonstrating 100% accuracy and sensitivity in medium- and large-sized patient models and 93-95% accuracy in obese-sized patient models. Figure 14 demonstrates the appearance of the software application, which color codes uric acid stones in red and non-uric acid stones in blue. The various types of non-uric acid stones (cystine, hydroxapatite, calcium oxalate, etc) contain higher atomic number elements and so distinguish themselves from the uric acid stones, which do not. Further development of the algorithm may allow differentiation between these non-uric acid stone types as well.



Conclusion

In summary, dual energy CT represents an emerging field of clinical CT imaging. The ability to differentiate material composition currently has several clinically-relevant applications, as described in this exhibit. Prospective clinical trials to evaluate the clinical efficacy of these techniques are underway, while ongoing research in the field is likely to yield additional clinical applications.

References

1. Macovski A, Alvarez RE, Chan R, Sorensen JM and Zatz LM. Energy dependent reconstruction in X-ray computerized tomography. *Comput Biol Med* 1976; 6: 325-36.
2. Alvarez RE, Macovski A. Energy-selective reconstructions in X-ray computerized tomography. *Phys Med Biol* 1976; 21: 733-44.
3. Kalender WA, Klotz E, Suess C. Vertebral bone mineral analysis: an integrated approach with CT. *Radiology* 1987; 164: 419-23.
4. Flohr TG, McCollough CH, Bruder H, Petersen M, Gruber K, Süss C, Grassack M, Sternbröker K, Krauss R, Raupach R, Primak AN, Kottner A, Achenbach S, Becker CR, Kopp A, Chenevigne B. First performance evaluation of a dual-source CT (DECT) system. *Eur Radiol* 2006; 16:256-265.
5. Johnson TR, Nikolaou K, Winteroppeger BL, Leber AW, von Ziegler F, Rist C, Baluwan S, Kner A, Reiser ME, Becker CR. Dual-source CT cardiac imaging: initial experience. *Eur Radiol*. 2006 Jul;16:1409-15.
6. Johnson TR, Krauss R, Sedlitz M, Grassack M, Bruder H, Mohr D, Fink C, Weiskopf S, Leber AW, Schmidt R, Flohr T, Reiser ME, Becker CR. Material differentiation by dual energy CT: Initial experience. *Eur Radiol*. 2007 Jun;17:1510-7.
7. Kalender WA, Klotz E, Kottner A. An algorithm for noise suppression in dual energy CT material density images. *IEEE* 1989; 7:218-224.
8. Primak AN, Fletcher JG, Vrtiska TJ, Dwyer DK, Laska JC, Jackson ME, Williams JC, McCollough CH. Non-invasive differentiation of uric acid versus non-uric acid kidney stones using dual-energy CT. *Acad Radiol* 2007; In Press.